Check for updates

Tidal variation modulates the dissolved silicate behavior and exchange flux across the semi-enclosed bay-coastal water continuum, China

Peng Zhang, Jiale Xie, Jibiao Zhang*, Miaojian Fu, Weisheng Luo and Mingyue Cheng

College of Chemistry and Environmental Science, Guangdong Ocean University, Zhanjiang, Guangdong, China

Coastal water is the key transition zone for the circulation and transport of nutrients. Their role in transporting nutrients is important to understanding global dissolved silicate (DSi) cycles and sources of nutrients supporting the biological pump and ocean carbon cycle. However, the understanding of controlling DSi exchange flux between the semi-enclosed bay and coastal water was still scarcely due to limitations in continuous observation. In this study, we conducted continuous investigations during spring tide (ST) and neap tide (NT) in 2021 in Shuidong Bay (SDB), China, to explore the impacts of different tidal cycles on DSi in SDB and the fluxes across SDB and South China Sea (SCS) coastal water. The findings demonstrated that there were significant differences in DSi concentrations and nutrients ratios between ST and NT in S1 station ($P < 0.05$). In addition, the DSi concentrations were 32.01 ± 27.21 µmol/L and 51.48 ± 48.44 µmol/L in ST and NT, respectively. Besides, the net export of DSi from SDB to SCS was 0.18 t throughout the entire early of autumn tidal cycle, suggesting SDB was the source of DSi, and its behavior across the semi-enclosed bay-coastal water continuum was largely controlled by tidal characteristics (tidal height, flow velocity), water physicochemical parameters (salinity, pH), biological uptake and terrestrial sources input. SDB in ST has higher proportions of DSi: DIN (dissolved inorganic nitrogen) (1.49 ± 1.28) and DSi: DIP (dissolved inorganic phosphorus) (58.6 ± 43.73) compared with NT, DSi: DIN and DSi: DIP for the NT period were 1.45 ± 1.15 and 43.99 ± 28.59, indicating that phosphorus (P) is the limiting trophic factor for SDB. The tidal cycle in SDB would alter the DSi stoichiometry and mitigated the impact of eutrophication caused by terrestrial sources. This study provides new insights in the Si tidal cycling across the semi-enclosed bay-coastal water continuum, which was implications for understanding DSi biogeochemical process and primary production dynamics in coastal water.

KEYWORDS

tidal variation, dissolved silicate, behavior, semi-enclosed bay, coastal water continuum

Abbreviations: DSi, Dissolved silicate; DIN, Dissolved inorganic nitrogen; DIP, Dissolved reactive phosphorus; Si, Silicon; N, Nitrogen; P, Phosphorus; SPM, Suspended particulate matter; SDB, Shuidong Bay; SCS, South China Sea; ST, Spring tide; NT, Neap tide.

Introduction

Silicon (Si) is a non-metallic element, which is one of the main components of seawater and the second most prevalent element in the Earth's crust after oxygen. Si is also found in both dissolved and particulate form in the ocean (Carey and Fulweiler, 2012). Si profoundly influences the surface material cycle and is one of the key elements in the study of surface processes, land-sea interactions, and the global carbon cycle (Zang et al., 2020). Si cycling is an important component of biogeochemical processes, and the surface runoff is the main sources of Si in the ocean, groundwater discharge, and sewage discharge (Zhu, 2017; Wang et al., 2023). Excessive nutrient levels cause eutrophication of water bodies and even natural calamities like red tides (Liu et al., 2011; Guo et al., 2012). Conversely, very low nutrient levels may cause disturbances in nutrient stoichiometry, hinder phytoplankton normal growth, and affect the balance of marine ecosystems (Bricker et al., 2003; Zhou, 2021). Dissolved silicate (DSi) is a crucial nutrient for diatom breeding (DeMaster, 1981; Papush et al., 2009; Cao et al., 2020). Diatom production accounts for more than 40% of the world's marine primary production, making them one of the most significant primary producers in the ocean (Song, 2010; Kranzler et al., 2019). Si played a key role in controlling the phytoplankton community (Officer and Ryther, 1980; Blanchard, 1988; Derry et al., 2005). Amorphous silica, also known as biogenic silica (BSi), is used by diatoms to build a silicified cell wall (Carbonnel et al., 2009; Wu and Liu, 2020). The amount of DSi that is available and how abundant it is in relation to other nutrients affects the make-up of the phytoplankton population and, consequently, the ecological efficiency of an ecosystem (Officer and Ryther, 1980; Conley et al., 1993; Turner et al., 2003; Carbonnel et al., 2009). In addition, the Si, combined with nitrogen (N) and phosphorus (P), which regulated planktonic blooms in aquatic ecosystems (Huang et al., 2019; Wu and Liu, 2020). Due to its intimate ties to the marine carbon cycle and biological pumps, the biogeochemical behavior and transport of Si has received much people's eyesight in recent years (Song et al., 2018; Sutton et al., 2018; Cao et al., 2020; Wu and Liu, 2020).

Under the climate change and human activities, the semi-enclosed bay-coastal water continuum has significantly impacted due to global warming, land-based sources input, land-reclamation and so on (Billen et al., 1991; Daniel et al., 2009; Zhang et al., 2017a). The coastal area is a key region for marine biogeochemical reactions, and ecological changes caused by human activities in the watershed are usually manifested in estuaries and bays (Ke et al., 2022). In addition, the bay's physicochemical properties, alters in the water column with tidal ebb and flow, and inputs of nutrients and organic matter are all significantly impacted by the tidal cycle. Natural factors such as geomorphic features, hydrodynamic conditions and water exchange cycles in estuarine bays influence their nutrient levels and eutrophication pattern (Cheng and Li, 2006). The circulation of water between estuaries and the outer sea, and predation by marine organisms also influence the eutrophication characteristics of estuaries, and therefore, the physical processes occurring here have important implications for biogeochemical reactions (Qu et al., 2007; Li et al., 2016; Li, 2021). Bays are one of the most eutrophic water habitats in the ocean and

the unique coastal weak exchange hydrodynamic environments, has experienced ecological deterioration under the impact of high-intensity human activities (Daniel et al., 2009; Wang, 2019; Li et al., 2020). In recent years, anthropogenic activities have had a major impact on the nutrients in bay water, increasing the amount of terrestrial nutrients entering coastal water (Santos et al., 2008; Amato et al., 2020). The stoichiometry and enrichment of nutrients in some coastal waters in China has gradually changed to some extent. From 2017 to 2019, the nitrogen and nitrogen-phosphorus limitations in Zhanjiang Bay were gradually replaced by phosphorus limitation (Zhou and Zhao, 2021); the silicate limitation in Jiaozhou Bay were gradually replaced by phosphorus limitation (Gao et al., 2018; Zhao et al., 2020); the Bohai Bay and Pearl River estuary's phosphorus limitation status deteriorated rapidly (Zhang et al., 2018; Ke et al., 2022); and Laizhou Bay experienced phosphorus limitation, which was particularly evident in flood period (You et al., 2021). Tidal changes, winds, convective dispersion, biological activity, and interaction at the water-sediment interface all have an impact on the distribution of Si in coastal waters (Pan and Shen, 2009). However, these studies have focused on the dynamic balance and cycling of Si, and the effects of tidal variations on the behavior and exchange flux of DSi has rarely been studied.

Tidal forces play an important role in regulating the dynamics of water-sediment in estuarine and coastal systems, including regulating water stratification, influencing freshwater and sediment funnel between rivers and bays, and further changing the dynamics of organic and inorganic components (Fang et al., 2008; Gao et al., 2009; Cheng et al., 2020). After terrestrial weathering of silicate minerals, large amounts of DSi flow into coastal waters with rivers (Billen et al., 1991; Tréguer and Rocha, 2013; Amann et al., 2014), and the riverine inflows provide approximately 80% of DSi to the world's seas (Sun and Song, 2001). These nutrients had various biogeochemical properties, and under the impact of tidal forces, they display various distributions, variations, and behaviors that further influence primary production. For example, the Venice Lagoon exported nitrogen and phosphorus to the Adriatic Sea while importing silicate (Ferrarin et al., 2013). Yuan et al. (2018) derived that Jiaozhou Bay exported DON and DOP to the Yellow Sea and imported DIN from the Yellow Sea. Therefore, a comparison of DSi concentrations and fluxes in the SDB with those in other coastal bays can provide insights into the similarities and differences between these coastal systems and their interactions with the open ocean. For example, the complex underwater environment and strong tidal mixing in San Francisco Bay have implications for the spatial and temporal distribution of suspended sediments and nutrients (Cloern et al., 2020). In addition, the sea surface temperature (SST) in the SCS and its coastal systems also changed in the context of global warming (Zhang et al., 2017b). The warming coastal water may trigger diatoms community, and then perturbed the DSi concentration dynamics. Therefore, studying the DSi dynamics in tidal cycle across the semi-enclosed bay-coastal water systems is important for a better understanding of DSi biogeochemical process in coastal water.

Shuidong Bay (SDB), as a semi-enclosed bay, is created when the Earth's crust slightly lifted (Liu, 2019; Cao, 2022). The bay's

mouth faces south and is encircled by a sizable sandbar. The bay is gently curved. The SDB marine dynamic environment is dominated by tidal currents (Yang et al., 2011), and its tidal type belongs to irregular semi-diurnal tides (Qin et al., 2014; Feng, 2017), i.e., there be two high tides and two low tides in a day, and the unequal tide levels and tidal times are obvious. Studies have shown that semi-diurnal tidal changes may significantly affect the dynamics of nutrients in SDB (Qin et al., 2014; Shi et al., 2017). Tides in SDB basically flow reciprocally along the tidal channel (Feng, 2017), and the special topographic and tidal variation characteristics of SDB largely determine the nutrient dynamics. In addition, the residence period of nutrients is determined by the hydrographic characteristics of coastal bays, and the combined impacts of surrounding seas further complicates the biogeochemical processes of the implicated nutrients (Hopkins et al., 1993; Li, 2021). Some nutrients may be absorbed or created during the movement of seawater as currents convey nutrients between SDB and SCS, resulting in increase or decrease nutrient concentrations in seawater during tidal fluctuations (Li, 2021). Numerous physical and biological elements, including microbial activity, terrestrial inputs, tidal forces, and primary generation in estuaries and seawater, affect the biogeochemical processes of nutrients (Dittmar and Lara, 2001; D'Croz and O'Dea, 2007; Guo et al., 2014). However, in recent years, with the rapid economic and social development, frequent human activities have exacerbated the decrease of exchange capacity and the occurrence of eutrophication of water bodies in the coastal waters of SDB, especially in estuarine bays (Li, 2011; Qin et al., 2014; Li et al., 2016; Feng, 2017; Zhang et al., 2022). Among them, the development of mariculture has directly disturbed the tidal pattern of the SDB, with a dramatic decrease in the exchange capacity of the water body and a serious deterioration of the water quality environment (Qin et al., 2014). Most of the available studies have concentrated on the mechanisms of tides and their effects on hydrodynamics (Song et al., 2011; Wu et al., 2011; Cheng et al., 2020), and the effects of estuarine physicochemical factors on phytoplankton and chlorophyll a (Niu et al., 2016) as well as only nutrients distribution patterns in coastal waters (Guo, 2020; Liu et al., 2021; Zhang et al., 2021; Ke et al., 2022). However, the natural environment and dynamic circumstances were been focused on in the earlier research in SDB, these studies lacked continuous measurements of DSi dynamics throughout the spring tide (ST) and neap tide (NT) cycles (Yang et al., 2020; Zhang et al., 2020c). At present, the DSi behavior, exchange flux, and controlling factors affected by different tidal cycles remains to be elucidated across the semi-enclosed bay-coastal water continuum, which is implications for understanding DSi biogeochemical process and primary production in coastal water.

Therefore, to better understand the effects of tidal variability on DSi, we concentrated on the temporal and spatial DSi variation and exchange flux in the SDB during the tidal period. We conducted periodic observations in the SDB-coastal water continuum during ST (22-23 August 2021) and NT (29-30 August 2021). Continuous interval observations of physicochemical parameters and shallow water samples were taken in the SDB during a ST-NT tidal cycle in 2021. The aims of this study were to: (1) investigate the cyclic and spatial variations in DSi concentration along the SDB-coastal water column continuum; (2) calculate DSi fluxes exchanged by the water column across the SDB and SCS; and (3) identify the major factors and processes that controlling the dynamic changes and transport patterns of DSi in the SDB during different tidal periods.

Materials and methods

Study areas

The study areas was located in SDB (111°0′-111°6′E, 21°27′-21°32′N), southwestern side of Maoming City, Guangdong Province (Figure 1). Approximately 32 Km^2 in size, SDB is a semi-enclosed bay with a wide water surface and a narrow sea mouth. The bay is long and oval in shape, oriented slightly to the southeast, with the mouth of the bay facing southeast. A 12.7 Km long, 500-800 m wide, and 5-15 m deep tidal channel connects the inner bay to the external SCS (Su et al., 2015). The symbols of R1 to R4 are the main seasonal major rivers adjacent to the bay. The topography of the bay bottom is complex with a clear distribution of grooves (Feng, 2017), and the bottom of the bay is muddy and sandy with high sedimentation and widespread subsidence (Su et al., 2015). Tidal
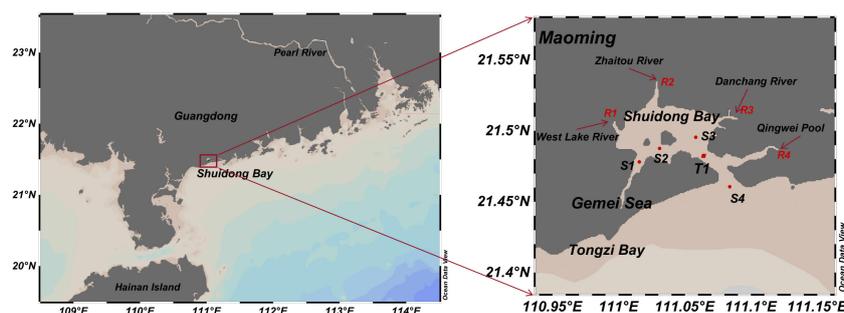

FIGURE 1
Geographic location and monitoring sites in the SDB.

action is the primary source of the SDB's hydrodynamic drive. The tidal characteristics of the SDB conform to the irregular semi-daily tide rule, with a maximum average flow velocity of 0.3-0.5 m/s and a maximum flow velocity of 1.0 m/s in the tidal channel (Qin et al., 2014). The mudflats and mangrove beaches are extensive within the SDB, with large saline areas along the coast (Cao, 2022). Recent years have seen the swift development of offshore aquaculture and increasing pollution from land-based sources have led to a reduction in the size of SDB waters and a deterioration in water quality, thus having a significant impact on the tidal patterns of the SDB (Li, 2011; Qin et al., 2014; Feng, 2017). According to the tidal characteristics and hydrological conditions of SDB, four distinct monitoring sites were chosen for this study to collect water samples at various periods during ST and NT. The methods standardized in the Marine Survey Code (General Administration of Quality Supervision, Inspection and Quarantine, People's Republic of China) were used to select the coastal water monitoring sites of the SDB, and the specific sampling sites are shown in Figure 1. Hydrological data for the SDB were obtained from Zhang et al. (2022), and specifications for different elements of nitrogen are cited in this study.

Field sampling and pre-treatment

Continuous 24-hour water sampling of the SDB was conducted during the ST (August 22-23, 2021) and NT (August 29-30, 2021) in early of autumn, respectively. A sampling period is divided into day (6:00 to 18:00) and night (18:00 to 6:00). Based on the shallow coastal consideration of the SDB, sampling was conducted from the surface layer at a depth of 0.5 m. The specific sampling method and water sample storage method refer to the study of Zhang et al. (2022). During this simultaneous survey cruise, four stations (S1, S2, S3, and S4) were deployed at sea for hydrodynamic and water quality monitoring. Hydrodynamic conditions were checked every 1 h and surface seawater samples were collected every 3 h for 24 hours of continuous monitoring. Prior to analyses, all samples were carefully collected, pre-processed, and stored in accordance with the methods standardized in the Marine Monitoring Code (GB17378-2007, AQSIQ, 2007b). The water samples need to be thawed before the measurement, so there should be sufficient time (preferably more than 24 hours) for depolymerization. The analysis of the water samples before and after freezing ensures that the freezing and thawing processes have no effect on the DSi content and that the results of the two measurements (10% of samples) are not significantly different.

Chemical analyses in the laboratory

DSi analysis was performed using the silicomolybdate blue spectrophotometric method, which has a detection limit of 0.03 μmol/L and a measurement blank of 0.002 μmol/L for DSi in water samples. A UV-Vis spectrophotometer (Shimadzu UV2600i) was used to measure the results of the aforementioned method at 812 nm. TN and TDN were analyzed by potassium persulfate oxidation. $N-NH_4^+$, $N-NO_3^-$ and $N-NO_2^-$ were performed using the

hypobromite oxidation, zinc-cadmium reduction, and diazo–azo methods, respectively. DIN was the sum of the concentrations of the above three components. The concentrations of DON (DON=TDN-DIN) and PN (PN=TN-TDN) were obtained indirectly by the method of making differences (Zhang et al., 2022). The phosphomolybdenum blue spectrophotometric method was used to analyze TP, TDP and DIP with the detection limit of 0.02 μmol/L at 882 nm. Similarly, the concentrations of DOP (DOP=TDP-DIP) and PP (PP=TP-TDP) were obtained indirectly by the differential method. Suspended particulate matter (SPM) was selected for measurement by weight method. Glass fiber membrane used in Chl-a filtration. Chl-a was measured using a spectrophotometric method. All of the above methods were estimated to have better than 5% relative deviation in repeatability, reproducibility and precision by duplicate measurements on 10% of the samples. All samples were strictly in accordance with the Marine Monitoring Code (GB17378-2007) to implement the whole process of monitoring quality control of collection - pretreatment - storage - analysis (AQSIQ, 2007a).

Estimation of the net flux of DSi in the tidal cycles

The SDB is closed on three sides, with only a narrow bay channel connecting the coastal waters to the SCS, S4 is designated to represent the DSi flux from the SDB gulf mouth to the SCS since it is near to the bay mouth while the other three stations are far away, and the specific directional division is referred to the study of Zhang et al. (2022). After designating the direction of flow to the SDB, the DSi flux transported between SCS and SDB was calculated with equations (1) and (2). The equation (1) calculates the water flux through S4 at different time. Then, the net DSi flux between the SDB and SCS was estimated by according to equation (2). The DSi net exchange flux between the SDB and SCS was approximately calculated at the cross sections of the bayport at different moments based on the variation of flow velocity at different moments, and then the DSi net exchange flux between the SDB and SCS was calculated for one day.

$$Q = W \times D \times V \qquad (1)$$

Where Q is the vector of net water flow rate (L/h) per unit time at the SDB port, W is width (m), D is depth (m), and V is flow rate at each time point (cm/s). All the above data refer to the data of S4.

$$F_{DSi} = C_{DSi} \times Q \times 10^{-6} \times M_{Si} \qquad (2)$$

Where F_{DSi} is the net exchange of DSi (t/h), C_{DSi} is the concentration of DSi at different moments (μmol/L), and M_{Si} is the relative atomic mass of silicon. All the above data refer to the data of the SDB port.

Statistical analyses

The normality of DSi concentrations between ST and NT was examined using K-S test (Kolmogorov-Smirnov test), if the results

demonstrate a normal distribution, an independent samples t-test was used, and if they did not demonstrate a normal distribution, a non-parametric Mann Whitney U test was then used for analysis to find significant differences between DSi specimens during ST and NT. Principal component analysis was performed on the major environmental factors and nutrients in SDB waters to determine the dominant factors affecting the DSi of SDB. To find the correlation between the dominant environmental factors, spearman correlation analysis was also performed. The relationship between ambient factor variables and various Si specimen concentrations was examined using Spearman correlation analysis (Zhang et al., 2020a). The link between DSi fluxes and flow rates during ST and NT was also examined using linear regression analyses. A significant difference between the variables is shown if *P < 0.05*.

Results

Dynamics of DSi in SDB in tidal cycles

There was no significant difference in DSi concentration between ST and NT in all stations ($p > 0.05$). DSi showed temporal and spatial variations in the SDB-coastal water continuum (Figure 2 and Table 1). Figure 2 showed the variation of DSi concentration with tidal height at the four stations of SDB. DSi concentrations during ST (Figure 2A) and NT (Figure 2B)

ranged from 4.48-108.31 μmol/L and 5.82-153.96 μmol/L, with mean concentrations of 32.01 ± 27.21 μmol/L and 51.48 ± 48.44 μmol/L, respectively. The DSi concentration peaked at 4:00 in S2 and the lowest at 10:00 in S2 during ST, and the DSi concentration peaked at 9:23 in S1 and the lowest at 14:26 in S2 during NT. DSi concentrations were lower in S1, S2, S3 and S4 at ST than at NT. Both during ST and NT, the mean values of DSi at SDB were S1 > S2 > S3 > S4; and the mean values of DSi at each station during ST were lower than those at each station during NT. The DSi concentrations and tides roughly showed a pattern of low DSi concentrations at ST and high DSi concentrations at NT on different time scales of ST and NT.

Nutrients ratios in SDB coastal waters during the tidal cycles

The DSi: DIN and DSi: DIP ratios were utilized to evaluate the temporal and spatial fluctuations of the nutrient stoichiometric balance in the bay in accordance with the tidal cycle and nutrient ratio variation patterns. The DSi: DIN and DSi: DIP varied with tidal cycles (Figure 3). There was a significant difference between DSi: DIN and DSi: DIP during ST and NT in S1 station ($P < 0.05$). DSi: DIN was closer for ST (1.49 ± 1.28) and NT (1.45 ± 1.15), while DSi: DIP differed more with 58.6 ± 43.73 and 43.99 ± 28.59. It was clear from Figure 3 that during the ST, the ratio of DSi: DIN exceeded 1 at all

FIGURE 2
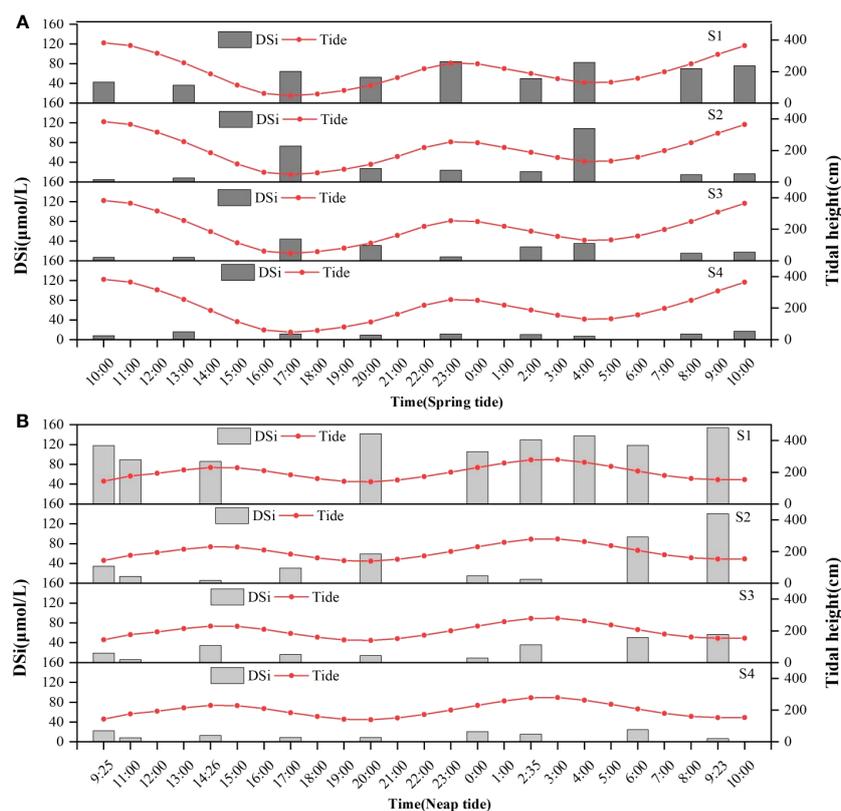DSi concentration and tidal height variation during spring tide **(A)** and neap tide **(B)**.

TABLE 1   Mean concentration of DSi at per station in SDB (µmol/L).

	S1		S2		S3		S4	
	ST	NT	ST	NT	ST	NT	ST	NT
DSi	62.11 ± 16.54	119.92 ± 22.01	33.07 ± 32.64	44.71 ± 43.06	21.53 ± 12.93	27.00 ± 17.22	11.31 ± 3.16	14.3 ± 6.33

moments except 10:00 and 7:00, and showed a regular trend of rising-falling- rising. The maximum value of DSi: DIN was 2.59, which occurred at 9:25 during the NT, and the minimum value was 0.69, which occurred at 11:00 during the NT. The ratio of DSi: DIP was significantly higher than 16 throughout the tidal cycle, with a general trend of increasing and then decreasing, and a wide range of variation. The maximum value of 92.53 and the minimum value of 25.92 occurred at 17:00 during ST and 11:00 during NT, and the average value of DSi: DIN during ST was 1.49 ± 1.28, which was 1.49 times of the reference value. The mean value of DSi: DIN during NT was 1.45 ± 1.15, which was 1.45 times of the reference value. DSi: DIP was 58.6 ± 43.73 during ST and 43.99 ± 28.59 during NT, which were 3.67 and 2.75 times of the reference value, respectively.

Net DSi flux of tidal cycles between SDB with SCS

The magnitude and direction of DSi fluxes varied with tidal cycles (Figure 4). There was a great variation in the net flux between SDB and SCS during ST and NT. During the ST of SDB (Figure 4A), DSi transported from SDB to SCS during half of the 24 h (11:00-17:00 and 24:00-4:00); while the rest of the time, DSi flowed from the SCS to the SDB. Since the DSi transport period from SDB to SCS accounts for half of the transport period and the DSi concentration was generally larger during ST, the total DSi transport from SDB to

SCS was larger than that from SCS to SDB, and the DSi exhibited an inflow from SDB to SCS. During NT of SDB (Figure 4B), SDB transported DSi to SCS during the time periods of 15:00-20:00 and 3:00-10:00, and during the rest of the time, SCS transported DSi to SDB. Although most of the time DSi transport was from SDB to SCS, the total DSi transport from SCS to SDB was higher than that from SDB to SCS, and DSi manifests itself as an inflow from SCS to SDB. At ST, DSi was the net export, and the daily efflux was 1.24 t. At NT, DSi was the net import, and the daily influx was 0.89 t. By counting the number of ST and NT days in SDB in early of autumn, it was calculated that the net exchange flux of DSi is expressed as input from SDB to SCS with a size of 0.18 t in the whole early of autumn tidal cycle.

Principal component analysis of DSi in SDB

Principal component analysis (PCA), as a variable reduction method, was applied to analyze the results of SDB water samples. The physicochemical variables included water physicochemical parameters (i.e., tide height, flow velocity, salinity, pH, and SPM), nutrients (i.e., N, P, and DSi), and Chl-*a*. PCA (Figure 5) showed relatively good repeatability between sites under ST conditions, indicating that the sample data were very similar. In contrast, there was a good variability between sites under NT conditions. This indicated that periodicity was the most important influencing factor
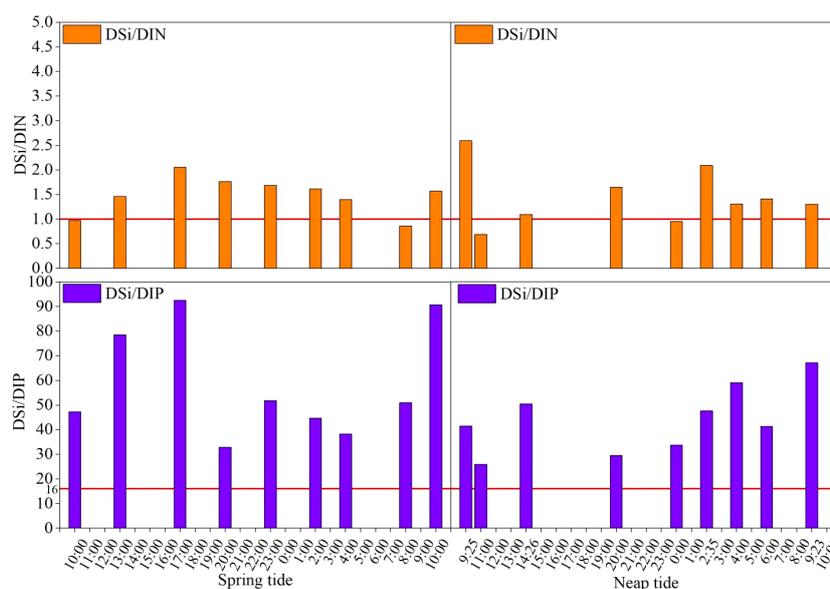

FIGURE 3
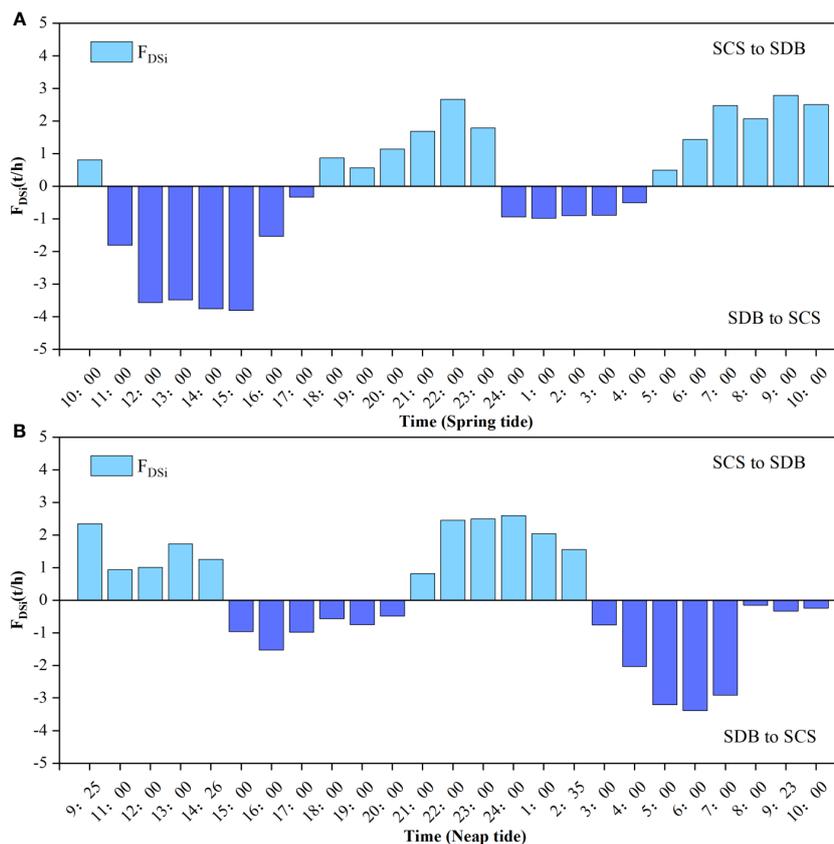Distinction of DSi: DIN and DSi: DIP during the tidal cycles in SDB.

FIGURE 4

DSi exchange flux of SDB and SCS during spring tide **(A)** and neap tide **(B)**.

under ST conditions. The spatial differences were more obvious under the NT conditions (Figures 2, 5). During ST, the first two axes (PC1 and PC2) accounted for 39.4% and 12.9% of the variation in SDB-related parameters, respectively (Figure 5A). DIP, Chl-*a* and DIN exhibited high positive DSi loadings, while salinity, pH and flow rate exhibited negative DSi loadings. It indicated that DSi may be positively correlated with DIP, Chl-*a* and DIN, and inversely correlated with salinity, pH and flow rate. DSi had some positive

correlation with sites S1 and S2, and weak correlation for site S3. In addition, different environmental factors and nutrient characteristics were evident during ST periods. clusters S1, S2 and S3 were separated by PC1, while PC2 separated cluster S4 from the other three clusters (Figure 5A). Analysis of water sample data from the NT showed that PC1 and PC2 covered 42.5% and 13.3% of the variation in water samples during NT, respectively. DIP, TDP and TP showed highly positive DSi loadings, while pH, flow velocity and
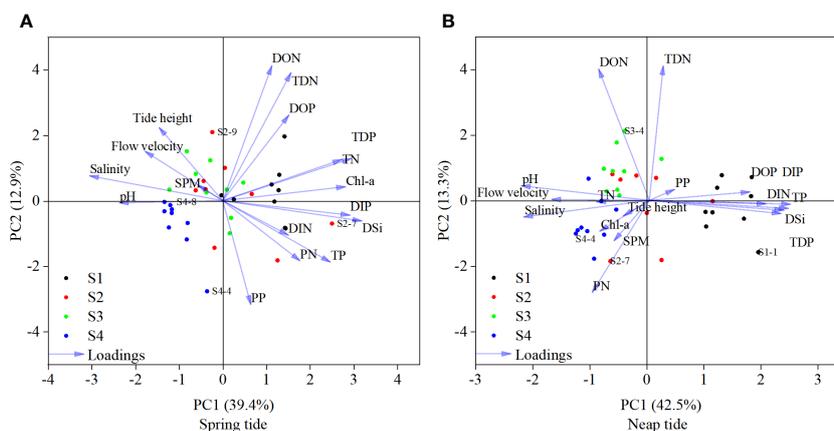

FIGURE 5

PCA considering the data collected during spring tide **(A)** and neap tide **(B)**.

TN showed negative DSi loadings, indicating that DSi may be positively correlated with DIP, TDP and TP and inversely correlated with pH, flow velocity and TN. DSi showed significant positive correlations with site S1 and weak negative correlations with the other three sites. In addition, the NT period also showed different environmental factors and nutrient characteristics. clusters S2 and S3 were separated by PC1 and separated cluster S1 from the other three clusters (Figure 5B). It was noteworthy that the positive load of DIP on DSi was the highest for both ST and NT periods, and the negative load of pH and flow velocity on DSi was higher. This indicated that DIP, pH and flow velocity may have a greater effect on DSi during both ST and NT periods. In general, the data dispersion of S2 was larger in both ST and NT conditions, indicating that several parameters had a greater impact on S2. The data in NT condition were more dispersed than those in ST condition.

Discussion

Comparison in DSi concentration in estuarine and coastal waters around the world

Table 2 showed the DSi concentrations in SDB with those in comparable semi-enclosed bays in China and other countries. The

results showed that the average DSi concentrations in SDB were 41.74 ± 40.48 µmol/L, which only lower than The western Bohai Bay (Wang et al., 2020), and much higher than those in Coastal waters of the northern Yellow Sea, Hangzhou Bay, Maumere Bay, and other estuaries and bays affected by human production and life (Gao et al., 2011; Zhang et al., 2020c; Meirinawati and Prayitno, 2021; Sun et al., 2022). In contrast, the mean DSi concentration in Maumere Bay was significantly lower than in other coastal waters with potential fishery resources (Meirinawati and Prayitno, 2021). In comparison, DSi concentrations were found to be relatively high in bays with aquaculture areas (Gao et al., 2011; Wang et al., 2020). The bays near economically developed areas, such as Shenzhen Bay, Hangzhou Bay, Bay of Bengal, the western Bohai Bay, Tokyo Bay and estuary, and San Francisco Bay, had relatively high DSi concentrations with wide range of concentrations. The combined comparisons indicated that human activities had an impact on DSi circulation (Kamatani and Takano, 1984; Gao et al., 2011; Satinder et al., 2015; Cloern et al., 2017; Wang et al., 2020; Tao et al., 2021). Both the mean DSi concentration and concentration range in winter were significantly lower than the data in this study (Fu et al., 2023), suggesting that the tidal driving effect on DSi in winter was not as pronounced as in early of autumn period. However, DSi concentrations in both seasons showed a similar trend of decreasing from the bay to the mouth of the bay. The SDB, as a semi-enclosed

TABLE 2 Comparison of DSi concentration between SDB and other bays and estuaries.

Study area	Survey time	Mean Concentration of DSi (µmol/L)	Range of DSi Concentration (µmol/L)	Reference
Shenzhen Bay	2016	—	1.18-174.64	Tao et al., 2021
Rongcheng Bay	2009	6.62	1.36-13.80	Xie et al., 2013
Hangzhou Bay	2006-2007	44.86	11.74-81.59	Gao et al., 2011
Caofeidian coastal water	2013.08-2014.05	—	0.71-9.52	Liu et al., 2020
Bay of Bengal	2014	—	0.6-152.5	Satinder et al., 2015
Daya Bay	2006.07-2007.11	13.20	—	Shi and Huang, 2013
The western Bohai Bay	2017	85.7± 9.52	74.6-95	Wang et al., 2020
Jiaozhou Bay	2013-2014	—	0.71-42.14	Gao et al., 2018
Maumere Bay	2017.08	4.54	—	Meirinawati and Prayitno, 2021
Laizhou Bay	2001	11.31	1.00-52.08	Sun et al., 2006
Coastal waters of the northern Yellow Sea (Aquaculture area)	2017	7.86 ± 0.78	—	Sun et al., 2022
Coastal waters of the northern Yellow Sea (Non-aquaculture area)	2017	7.77 ± 1.25	—	Sun et al., 2022
Tokyo Bay and estuary	1979-1980	—	10-300	Kamatani and Takano, 1984
San Francisco Bay	1988–2015	—	25-275	Cloern et al., 2017
Zhanjiang Bay (Coastal water)	2019	20.86 ± 13.14	3.57–56.42	Zhang et al., 2020c
SDB	2021.01	6.15 ± 1.37	3.75-10.36	Fu et al., 2023
SDB	2021.08	41.74 ± 40.48	4.48-153.96	This study

"—" means not detected.

bay, had only a narrow bay channel connected to the water exchange in the SCS, causing to difficulties in the exchange of the internal and external circulation in the inlet (Zhang, 2015; Feng, 2017). Due to the estuary's long-term deposit of pollutants, which cannot be diffused and diluted, the land coastal areas of the bay were more abundant in DSi than near the bay mouth.

Modulation of DSi dynamics by coastal hydrodynamics due to tidal variations

Figure 6 demonstrated that DSi and salinity exhibited a strong connection during both ST and NT($P < 0.01$). Furthermore, linear fitting of DSi concentration and salinity (Figure 7) revealed a linear

decreasing relationship between DSi and salinity during ST; while the relationship between DSi and salinity during NT was more in line relationship with the nonlinear model. During NT, DSi varied more when the salinity was below 25‰ and less when the salinity was above 25‰. This suggests that salinity around 25‰ during NT is a turning point in the magnitude of DSi variation. Studies have concluded that tides are a key factor in regulating the transport of materials from rivers and oceans to coastal areas (Montani et al., 1998; Cheng and Li, 2006; Fernandes et al., 2021). The findings of the correlation study between environmental parameters and DSi at ST and NT, respectively, are displayed in Figures 6A, B. The results showed that a highly significant negative correlation ($P < 0.01$) was between DSi concentration and salinity and flow velocity during ST and NT, indicating that physical mixing may be the main factor
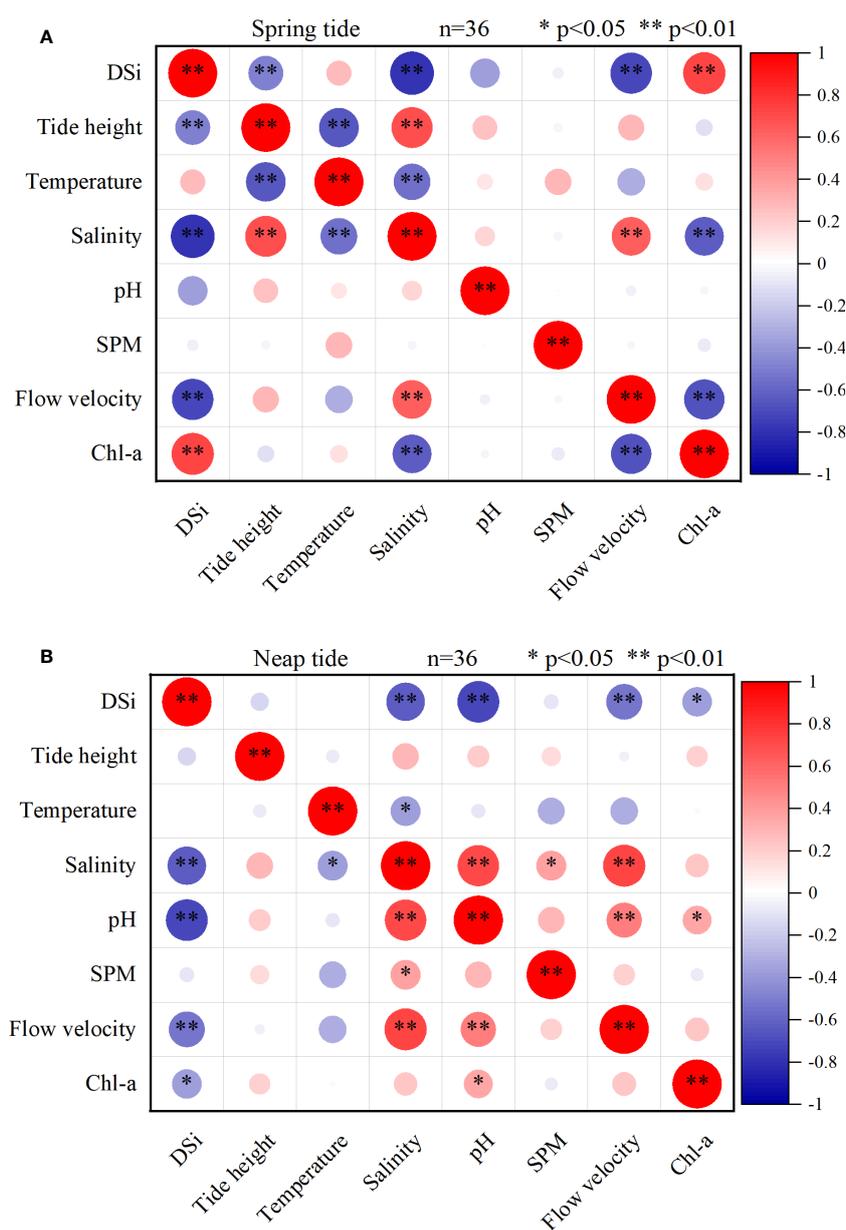

FIGURE 6
Correlation coefficients between SDB hydrological conditions and DSi concentration during spring tide (A) and neap tide (B).
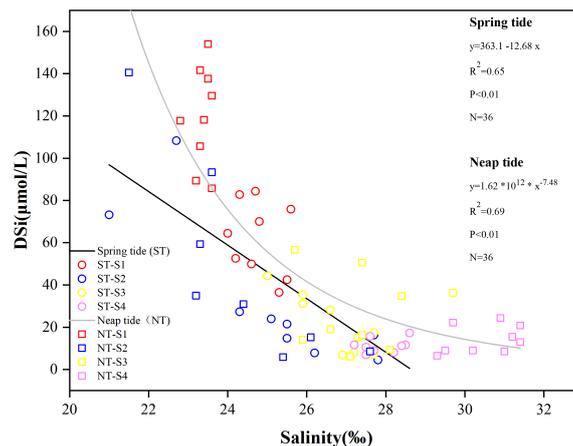
FIGURE 7
Linear regression analysis of DSi with salinity.

influencing the tidal variation of DSi, and its distribution was mainly influenced by the strong mixing effect of the outer ocean currents and their mutual extinction (Ren, 2019). Freshwater runoff also strongly affected the salinity of the estuarine surface layer (Montani et al., 1998; Lee et al., 2018). Uncles and Stephens (1996) found that saline water intrusion was slightly connected to freshwater inflow and highly correlated with tidal state. The flow velocity at ST was significantly greater than that at NT, and the greater the variation in flow velocity, the stronger the turbulence effect in the water column and the more pronounced the effect on nutrients (Ren, 2019). Increased flow velocities cause enhanced mixing of the water column. Particulate organic matter precipitated and was thus degraded by bacteria when the flow velocity decreases (Yin and Harrison, 2000). At the same time, the resuspension of sediments drastically altered the chemical stoichiometry of the overlying water column, releasing nutrients that required for planktonic life activities (Bancon-Montigny et al., 2019; Fernandes et al., 2021).

At ST, there was a significant positive correlation between DSi concentration and Chl-*a* concentration (*P < 0.01*), while at NT, there was a negative correlation (*P < 0.05*). Greater variability is allowed under ST conditions, as stronger seawater-river variability affects water quality parameters and phytoplankton biomass may increase due to resuspension of benthic communities (Biguino et al., 2021). The results suggesting that in addition to DSi dynamics being controlled by water exchange and chemisorption or desorption processes (Dilorenzo et al., 2004; Cloern et al., 2017), diatom and plant root uptake may also contribute to DSi (Kamatani and Takano, 1984; Wang et al., 2023). Although DSi fluxes at ST were substantially larger than at NT, DSi concentrations were lower. This may be due to the large number of mayfly organisms and diatoms brought in by ST, whose biosorption and release of DSi affect DSi concentrations (Blanchard, 1988; Song, 2010), while groundwater discharge from mangrove sediments affected DSi concentration in NT (Wang et al., 2023). The SDB was a tidally powered lagoon whose dynamic characteristics were driven by offshore tidal currents (Gan et al., 2006) and there were few river confluences

nearby. At ST, there was a strong correlation between DSi concentration and tidal height (*P < 0.01*), and it can be speculated that seawater played a dominant role with a large range of tidal height variation and significant tidal level change at ST (Wang et al., 2023). The phytoplankton in SDB was dominated by diatoms, which grow well in low temperature, low salinity and high nitrogen-phosphorus ratio (Shi et al., 2017). SDB is located in the subtropical zone with favorable water temperature. During the ST period, due to the influence of tides and waves, strong mixing occurred in the surface and bottom waters of the bay, and the water level dropped, which brought the diatoms favoring benthic life to the planktonic community, and these algae were in the competitive advantage of growth and reproduced in large quantities under the suitable environmental conditions, thus inhibiting the survival space of other species and becoming the dominant population. While the water exchange in the bay was smooth during the NT period, a large amount of foreign seawater influxed, the mixing of benthic diatoms weakened, and their dominance decreased accordingly (Su et al., 2015; Shi et al., 2017). And the poor water permeability in the SDB due to harbor transportation, aquaculture, and littoral currents affects the photosynthesis of the organisms, resulting in a lower biomass in the bay (Li, 2011; Yang et al., 2011; Qin et al., 2014). Longitudinal tidal advection was an important process controlling nutrient distribution in the coastland (Dilorenzo et al., 2004). Changes in tide levels caused longitudinal tidal advection, which in turn affected the distribution of nutrients. Since there was a large amount of seawater exchange between SDB and SCS, and the large amount of seawater exchange had a significant dilution effect on DSi concentration, resulting in the variation of DSi concentration with seawater exchange. In other words, there was a certain variation relationship between DSi and tide level. In previous research, it was discovered that the concentration of DSi increases with decreasing pH when the pH is between 4 and 9 (Qin and Weng, 2006). The significant negative correlation between DSi and pH at NT (*P < 0.01*) showed pH strongly affects Si dissolution. This could be as a result of the significant DSi absorption by phytoplankton during photosynthesis

(Qu et al., 2006), resulting in a significant increase in pH in the water column. In addition, the pH had an impact on the release of weakly bound Si (Kellermeier et al., 2012). In contrast, the frequent seawater exchange between SDB and SCS during ST and mangrove roots absorb acid ions from sediments (Wang et al., 2023) leaded to a stabilization of pH and DSi in the bay, so that the relationship between DSi concentration and pH during ST did not show a significant relationship.

Implications for tidal cycle on nutrients composition in SDB coastal waters

Previous researches have shown that the level and structure of nutrients had a significant impact on phytoplankton blooms in coastal waters (Zhang et al., 2020b; Zhang et al., 2019). In nutrient-balanced and sufficient populations, the Si:N:P ratio of marine diatoms was around 16:16:1 (Redfield et al., 1963; Brzezinski, 1985; Danielsson et al., 2008; Maguire and Fulweiler, 2017). Therefore, the ratios of DSi: DIN and DSi: DIP should be lower than 1 and 16, respectively, which also indicates the potential limiting effect of DSi on diatom populations growth. Alters in nutrient stoichiometry maybe have a negative influence on the ecology in coastal waters (Brzezinski, 1985; Fisher et al., 1992; Danielsson et al., 2008). The mean ratios of DSi: DIN and DSi: DIP in coastal waters of the SDB were 1.49 ± 1.28 and 58.60 ± 43.73 at ST; The mean ratios of DSi: DIN and DSi: DIP at NT were 1.45 ± 1.15 and 43.99 ± 28.59. The ratios of DSi: DIN and DSi: DIP were higher than the Redfield ratios, suggesting that Si was not limited in the studied region in comparison to Nitrogen (N) and P (Figure 3) and that the SDB falls within a severe phosphorus depletion zone. This was consistent with the conclusion of Guo et al. (1998) that the major estuaries and bays offshore China are generally at phosphorus-limited or moderately phosphorus-limited levels of potential eutrophication. In addition, DSi: DIN and DSi: DIP ratios showed significant tidal cyclic distinctions in S1 station ($P < 0.05$). The ratios of DSi: DIN was higher at ST (1.49 ± 1.28) than at NT (1.45 ± 1.15), and the DSi: DIP ratio showed the same trend of tidal periodicity. These nutrient loading discrepancies might result in varied nutritional conditions for phytoplankton breeding (Lee et al., 2018). The discharge of nutrient-rich production and domestic wastewater had been a crucial factor disturbing the stability of the bay-coast system. Biogeochemical cycling together with influent components from estuaries and sewage outfalls can led to increases in DSi: DIN and DSi: DIP, which had a sizable effect on the nutrient stoichiometry of SDB coastal waters. This might be one of the essential reasons why riverine inputs regulate the nutrient ratios in coastal waters (Montani et al., 1998; Zhang et al., 2019). Eutrophication of SDB coastal waters, increased primary production and colonization of diatom communities caused an increase in DSi: DIN and DSi: DIP from terrestrial sources. Previous studies have demonstrated that P enrichment increases diatom production and depletes DSi reserves in the water, resulting in DSi-limited diatom growth (Conley et al., 1993). Significantly low P

levels in the SDB may limit diatom production, resulting in significant DSi accumulation. Under the diatom-driven diatom biopump, which is distinguished by rapid proliferation rates and high nutritional demand (Raguneau et al., 2006; Cao et al., 2020). Eutrophication was not the only environmental factor that induces red tides; nutrient ratios also frequently regulate algal cell growth, phytoplankton diversity and abundance, leading to the occurrence of red tides, which in turn destabilize marine ecosystems (Humborg et al., 1997; Han et al., 2003; Garnier et al., 2010; Lin and Lin, 2022). Therefore, adjusting the trophic structure of SDB is the key to reduce the occurrence of red tide in the region.

Factors controlling the flux of DSi through the SDB-SCS

Figure 8 showed the relationship between DSi flux and flow rate during ST and NT. The direction of water flow into SDB is specified to be positive, and if the flow rate > 0, the SCS transports exchange flux to the SDB; conversely, the SDB transports exchange flux to the SCS. The results showed a significant relationship between flow rate and DSi flux. During ST and NT in the SDB, there was an extremely significantly negative correlation between F_{DSi} and flow velocity ($P < 0.01$) during ST and was a significantly negative correlation between F_{DSi} and flow velocity ($P < 0.05$) during NT when SDB transports DSi net flux to SCS. When SCS transports DSi net flux to SDB, there was an extremely significantly negative correlation between F_{DSi} and flow velocity during ST ($P < 0.01$) and was a significantly negative correlation between F_{DSi} and flow velocity during NT ($P < 0.05$). Changes in flow velocity led to changes in current direction and material concentration (Cheng and Li, 2006; Li et al., 2016), which in turn led to tidal cycle changes in DSi concentration. While the high concentration of DSi in SDB is caused by the discharge from land-based DSi sources, the high flow rate from SDB to SCS makes the flux of DSi between SDB and SCS increase significantly. Gao et al. (2009) suggested that the tidal variation of SPM concentration is an critical factor affecting nutrient levels in the Yangtze estuary. The tidal variation of DSi in SDB may be similar to that of the Yangtze estuary. Upper shore surfaces were disturbed by wave deformation and fragmentation, which affected sediment distribution (Yu and Chen, 2010), most particulate organic matter was produced at NT and trapped in the estuary, and channel sinuosity and the resuspension of sediment from bottom to surface influence DSi changes (Fernandes et al., 2021). Hydraulic conditions affected the velocity of coastal seawater passage through the open ocean and the bay, resulting in net exchange flux input and output of DSi on the day. During the winter ST period, DSi is transported from the SDB to the SCS (Fu et al., 2023), which is consistent with DSi transport during the ST period in this study. It was noteworthy that the different directions of nutrient transport between the Venice Lagoon and the Adriatic Sea do not coincide (Ferrarin et al., 2013). This may indicate that tidal variations had different effects on biogeochemical processes in different coastal ecosystems.
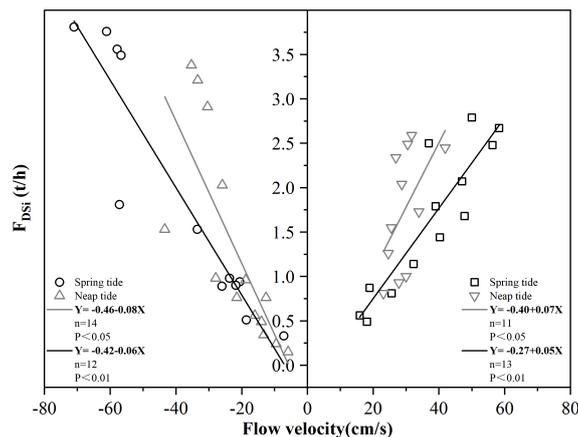
FIGURE 8
Linear regression analysis of F_{DSi} with flow velocity.

The findings revealed that the concentration of DSi in SDB had a distinct temporal and spatial distribution characteristic over the investigation period. During ST and NT, DSi concentrations at the four stations presented a rise trend from the estuary to the bay. The DSi concentration varies from station to station, and stations with high DSi concentration were distributed within the bay. It was possible that the proximity of human activities in the bay to local living and breeding seas has led to increased DSi concentrations in the water (Li, 2011). In contrast, the SDB is a semi-enclosed bay linked to the SCS by a narrow tidal channel. Long and narrow bays tend to have weak hydrodynamic conditions within the bay due to the small width and long depth of the inlet (Zhang, 2015). There was a large amount of seawater exchange from the SCS at the coastal mouth, and the frequent seawater exchange results in low and fluctuating DSi concentrations. Ocean currents had the greatest impact on coastal waters. As SDB and SCS exchange tidal currents across the mouth of the bay, dilute mixing of SDB seawater occurred (Béjaoui et al., 2017; Bancon-Montigny et al., 2019). Previous studies at Sado estuary and the Yangtze River estuary shown that enhanced seawater exchange capacity play a significant dilution role, thereby alleviating nutrient enrichment in semi-enclosed bays (Cereja et al., 2022; Song et al., 2022).

Conclusions

In summary, this study explores that tidal variation modulates the dissolved silicate behavior and exchange flux across the semi-enclosed bay-coastal water continuum by time series observations. The findings show there were significant differences in DSi concentrations and nutrients ratios between spring tide and neap tide in S1 station. In addition, DSi behavior and exchange flux across the semi-enclosed bay-coastal water continuum was largely controlled by tidal characteristics (tidal height, flow velocity), water physicochemical parameters (salinity, pH), biological uptake and terrestrial sources input. Furthermore, the DSi concentrations in the

SDB during ST and NT were 32.01 ± 27.21 µmol/L and 51.48 ± 48.44 µmol/L, respectively, which were at a high level compared to the bays near economically developed regions around the world. The significantly high DSi: DIP ratio (58.6 ± 43.73 in ST and 43.99 ± 28.59 in NT) indicates that P is the limiting trophic factor in the SDB. The spatial and temporal distribution of DSi and the fluxes across the SDB-SCS indicate that the SDB is the source of DSi. The net export of DSi from SDB to SCS was 0.18 t throughout the entire early of autumn tidal cycle. Besides, tidal cycle in SDB will alter the stoichiometry of DSi and mitigate the effects of eutrophication in the bay due to land-based inputs, which may regulate phytoplankton biomass and community in coastal water. This study sheds new light on the effects of tidal changes on Si cycling in a semi-enclosed bay-coastal water continuum. Future studies of other bay-coastal water bodies continuum are recommended to explore the regional long-term effects of tidal changes on Si biogeochemical cycling and ecological effects.

Data availability statement

The original contributions presented in the study are included in the article/Supplementary Material. Further inquiries can be directed to the corresponding author.

Author contributions

Funding

Acknowledgments

Conflict of interest

The authors declare that the research was conducted in the absence of any commercial or financial relationships that could be construed as a potential conflict of interest.

Publisher's note

All claims expressed in this article are solely those of the authors and do not necessarily represent those of their affiliated organizations, or those of the publisher, the editors and the reviewers. Any product that may be evaluated in this article, or claim that may be made by its manufacturer, is not guaranteed or endorsed by the publisher.

Supplementary material

The Supplementary Material for this article can be found online at: https://www.frontiersin.org/articles/10.3389/fmars.2023.1229267/full#supplementary-material

References

Amann, T., Weiss, A., and Hartmann, J. (2014). Silica fluxes in the inner Elbe estuary, Germany. *Biogeochemistry* 118, 1–24. doi: 10.1007/s10533-013-9940-3

Amato, H. K., Wong, N. M., and Pelc, C. (2020). Effects of concentrated poultry operations and cropland manure application on anti- biotic resistant escherichia coli and nutrient pollution in Chesapeake Bay watersheds. *Sci Total. Environ.* 735 (15), 1–11. doi: 10.1016/j.scitotenv.2020.139401

AQSIQ (2007a). *Specifications for oceanographic surey-part 4: Survey of chemical parameters in sea water (GB/T 12764.4-2-7)* (Beijing: Standards Press of China).

AQSIQ (2007b). *The specification for marine monitoring-part 4: Seawater analysis (GB 17378.4-2007)* (Beijing: Standards Press of China).

Bancon-Montigny, C., Gonzalez, C., Delpoux, S., Avenzac, M., Spinelli, S., Mhadhbi, T., et al. (2019). Seasonal changes of chemical contamination in coastal waters during sediment resuspension. *CHEMOSPHERE* 235, 651–661. doi: 10.1016/j.chemosphere.2019.06.213

Béjaoui, B. C. S., Harzallah, A., Chevalier, C., Chapelle, A., Zaaboub, N., and Aleya, L. (2017). 3D modeling of phytoplankton seasonal variation and nutrient budget in a southern Mediterranean lagoon. *Mar. Pollut. Bull.* 114 (2), 962–976. doi: 10.1016/j.marpolbul.2016.11.001

Biguino, B., Borges, C., Rui, C., and Brito, A. (2021). Tidal variability of water quality parameters in a mesotidal estuary (sado estuary, Portugal). *Sci. Rep.* 11, 23112. doi: 10.1038/s41598-021-02603-6

Billen, G., Lancelot, C., and Meybeck, M. (1991). "N, P, and Si retention along the aquatic continuum from land to ocean," in *Ocean Margin Processes in Global Change, Mantoua*. Eds. F. C. R., J. M. Martin and R. Wollast (New York, NY, USA: Wiley), 19–44.

Blanchard, S. F. (1988). *Dissolved Silica in the Tidal Potomac River and Estuary 1979-81 Water Years. (Water Supply Paper 2234-H)* (Denver, CO, USA: United States Geological Survey), 46.

Bricker, S. B., Ferreira, J. G., and Simas, T. (2003). An integrated methodology for assessment of estuarine trophic status. *Ecol. Model.* 169 (1), 39–60. doi: 10.1016/S0304-3800(03)00199-6

Brzezinski, M. A. (1985). The Si: C: N ratio of marine diatoms: Interspecific variability and the effect of some environmental variables. *J. Phycol.* 21, 347–357. doi: 10.1111/j.0022-3646.1985.00347.x

Cao, S. Y. (2022). Exploration of ecological restoration strategy of Shuidong Bay lagoon under the construction of beautiful bay. *J. Green Sci. Technol.* 22, 64–68. doi: 10.16663/j.cnki.lskj.2022.22.025

Cao, Z. M., Wang, D. N., Zhang, Z. L., Zhou, K. B., Liu, X., Wang, L., et al. (2020). Seasonal dynamics and export of biogenic silica in the upper water column of a large marginal sea, the northern South China Sea. *Prog. Oceanogr.* 188, 102421. doi: 10.1016/j.pocean.2020.102421

Carbonnel, V., Lionard, M., Muylaert, K., and Lei, C. (2009). Dynamics of dissolved and biogenic silica in the freshwater reaches of a macrotidal estuary (The Scheldt, Belgium). *Biogeochemistry* 96 (1-3), 49–72. doi: 10.1007/s10533-009-9344-6

Carey, J. C., and Fulweiler, R. W. (2012). Human activities directly alter watershed dissolved silica fluxes. *Biogeochemistry* 111, 125–138. doi: 10.1007/s10533-011-9671-2

Cereja, R., Brotas, V., Nunes, S., Rodrigues, M., Cruz, J. P., and Brito, A. C. (2022). Tidal influence on water quality indicators in a temperate mesotidal estuary (Tagus Estuary, Portugal). *Ecol. Indicat.* 136, 108715. doi: 10.1016/j.ecolind.2022.108715

Cheng, X. Y., and Li, S. J. (2006). An analysis on the evolvement processes of lake eutrophication and their characteristics of the typical lakes in the middle and lower reaches of Yangtze River. *Chin. Sci. Bull.* 51, 1603–1613. doi: 10.1007/s11434-006-2005-4

Cheng, P., Yu, F., Chen, N., and Wang, A. (2020). Observational study of tidal mixing asymmetry and eddy viscosity-shear covariance-induced residual flow in the Jiulong River estuary. *Cont. Shelf. Res.* 193, 104035. doi: 10.1016/j.csr.2019.104035

Cloern, J. E., Jassby, A. D., Schraga, T. S., Nejad, E., and Martin, C. (2017). Ecosystem variability along the estuarine salinity gradient: Examples from long-term study of San Francisco Bay. *Limnol. Oceanogr.* 62, S272–S291. doi: 10.1002/lno.10537

Cloern, J. E., Schraga, T. S., Nejad, E., and Martin, C. (2020). Nutrient status of San Francisco bay and its management implications. *Estuar. Coast.* 43 (6), 1299–1317. doi: 10.1007/s12237-020-00737-w

Conley, D. J., Schelske, C. L., and Stoermer, E. F. (1993). Modification of the biogeochemical cycle of silica with eutrophication. *Mar. Ecol. Prog. Ser.* 101, 179–192. doi: 10.3354/meps101179

Daniel, J. C., Hans, W. P., and Rober, W. H. (2009). Controlling eutrophication: nitrogen and phosphorus. *Science* 323, 1014–1015. doi: 10.1126/science.1167755

Danielsson, Å., Papush, L., and Rahm, L. (2008). Changing the Baltic Sea as a consequence of alterations in nutrient limitations. *J. Mar. Syst.* 73, 263–283. doi: 10.1016/j.jmarsys.2007.10.015

D'Croz, L., and O'Dea, A. (2007). Variability in upwelling along the Pacific shelf of Panama and implications for the distribution of nutrients and chlorophyll. *Estuar. Coast. Shelf. S.* 73 (1-2), 325–340. doi: 10.1016/j.ecss.2007.01.013

DeMaster, D. J. (1981). The supply and accumulation of silica in the marine environment. *Geochim. Cosmochim. Acta* 45 (10), 1715–1732. doi: 10.1016/0016-7037(81)90006-5

Derry, L. A., Kurtz, A. C., Ziegler, K., and Chadwick, O. A. (2005). Biological control of terrestrial silica cycling and export fluxes to watersheds. *Nature* 433, 728–731. doi: 10.1038/nature03299

Dilorenzo, J. L., Filadelfo, R. J., Surak, C. R., Litwack, H. S., Gunawardana, V. K., and Najarian, T. O. (2004). Tidal variability in the water quality of an urbanized estuary. *Estuar. Coast.* 27 (5), 851–860. doi: 10.1007/BF02912046

Dittmar, T., and Lara, R. J. (2001). Driving forces behind nutrient and organic matter dynamics in a mangrove tidal creek in North Brazil. *Estuar. Coast. Shelf. S.* 52 (2), 249–259. doi: 10.1006/ecss.2000.0743

Fang, T., Li, D. J., Kong, D. J., Yu, L. H., Li, Y., Gao, L., et al. (2008). Distribution of N and P nutrients and their tidal variations in the Yangtze River estuary and adjacent waters in summer and autumn. *Mar. Environ. Sci.* 5, 437–442. doi: 10.3969/j.issn.1007-6336.2008.05.009

Feng, S. J. (2017). Characterization and 3D numerical simulation of tidal currents in Shuidong bay. *J. Appl. Oceanogr.* 36 (3), 333–340. doi: 10.3969/J.ISSN.2095-4972.2017.03.005

Fernandes, L. L., Kessarkar, P. M., Dhandayudapani, I., Narvekar, J., Suresh, S., and Parab, P. (2021). Seasonal and tidal variations in suspended particulate matter dynamics of two microtidal rivers of karnataka, central west-coast of India. *Arab. J. Geosci.* 14 (18), 1–19. doi: 10.1007/s12517-021-08193-x

Ferrarin, C., Ghezzo, M., Umgiesser, G., Tagliapietra, D., Camatti, E., Zaggia, L., et al. (2013). Assessing hydrological effects of human interventions on coastal systems: numerical applications to the Venice Lagoon. *Hydrol. Earth Syst. Sci.* 17 (5), 1733–1748. doi: 10.5194/hess-17-1733-2013

Fisher, T. R., Peele, E. R., Ammerman, J. W., and Harding, L. W.Jr. (1992). Nutrient limitation of phytoplankton in Chesapeake Bay. *Mar. Ecol. Prog. Ser.* 82 (1), 51–63. doi: 10.3354/meps082051

Fu, M. J., Lin, J. L., Zhang, P., Luo, W. L., and Zhang, J. B. (2023). Tide drives nutrients variation and exchange flux in the semi-enclosed Shuidong Bay coastal water in winter, South China Sea. *Ocean. Coast. Manage.* 242, 106710. doi: 10.1016/j.ocecoaman.2023.106710

Gan, G., Zhu, S. H., Huang, B. F., and Hu, L. H. (2006). Environmental impact prediction of sewage discharge from Shuidong Harbor Bay. *Guangdong Water Resour. Hydropower.* 6, 23–25. doi: 10.3969/j.issn.1008-0112.2006.06.009

Gao, S. Q., Chen, J. F., Jin, H. Y., Wang, K., Lu, Y., Li, H. L., et al. (2011). Characteristics of nutrients and eutrophication in the Hangzhou Bay and its adjacent waters. *J. Mar. Sci.* 29, 36–46. doi: 10.3969/j.issn.1001-909X.2011.03.005

Gao, L., Li, D. J., and Ding, P. X. (2009). Quasi-simultaneous observation of currents, salinity and nutrients in the Changjiang (Yangtze River) plume on the tidal timescale. *J. Mar. Systems.: J. Mar. Sci. Tech-Japan.* 75 (1-2), 265–279. doi: 10.1016/j.jmarsys.2008.10.006

Gao, L., Zhang, M. M., Yao, H. Y., Liu, Y. L., Jiang, H. H., and Sha, J. J. (2018). An analysis of nutrient structure and limitation changes in Jiaozhou Bay in recent years. *Trans. Oceanol. Limnol.* 6, 61–68. doi: 10.13984/j.cnki.cn37-1141.2018.06.009

Garnier, J. A., Mounier, E. M., Laverman, A. M., and Billen, G. F. (2010). Potential denitrification and nitrous oxide production in the sediments of the Seine River drainage network (France). *J. Environ. Qual.* 39 (2), 449–459. doi: 10.2134/jeq2009.0299

Guo, J. (2020). *Nitrogen biogeochemical processes and nutrient deposition records in the nearshore waters of beibu gulf, guangxi* (Naning: Guangxi University).

Guo, Z. H., Wang, C., Yan, L., and Wang, J. K. (2012). Spatial and temporal variation characteristics of major pollutants in the Jiulong River estuary. *China Environ. Sci.* 32 (4), 679–686. doi: 10.3969/j.issn.1000-6923.2012.04.017

Guo, W., Yang, L., Zhai, W., Chen, W., Osburn, C. L., Huang, X., et al. (2014). Runoff- mediated seasonal oscillation in the dynamics of dissolved organic matter in different branches of a large bifurcated estuary- The Changjiang Estuary. *J. Geophys. Res. Biogeo.* 119 (5), 776–793. doi: 10.1002/2013JG002540

Guo, W. D., Zhang, X. M., Yang, Y. P., and Hu, M. H. (1998). Evaluation of the degree of potential eutrophication in China's nearshore waters. *J. Appl. Oceanogr.* 1, 64–70. doi: 10.1088/0256-307X/15/3/016

Han, X. R., Wang, X. L., Sun, X., Shi, X. Y., Zhu, C. J., Zhang, C. S., et al. (2003). Nutrient distribution and its relationship with occurrence of red tide in coastal area of East China Sea. *J. Appl. Ecol.* 14 (7), 1097–1101. doi: 1013287/j.1001—9332.2003.0245

Hopkins, J. S., Hamilton, R. D., Sandifer, P. A., Browdy, C. L., and Stokes, A. D. (1993). Effect of water exchange rate on production, water quality, effluent characteristics and nitrogen budgets of intensive shrimp ponds. *J. World. Aquacult. Soc* 24, 304–320. doi: 10.1111/j.1749-7345.1993.tb00162.x

Huang, Y. B., Mi, W. J., Hu, Z. Y., and Bi, Y. H. (2019). Effects of the Three Gorges Dam on spatiotemporal distribution of silicon in the tributary: Evidence from the Xiangxi River. *Environ. Sci. Pollut. Res.* 26, 4645–4653. doi: 10.1007/s11356-018-3707-2

Humborg, C., Ittekkot, V., Cociasu, A., and Bodungen, B. V. (1997). Effect of danube river dam on black sea biogeochemistry and ecosystem structure. *Nature* 386 (6623), 385–388. doi: 10.1038/386385a0

Kamatani, A., and Takano, M. (1984). The behavior of dissolved silica during the mixing of river and sea waters in Tokyo Bay. *Estuar. Coast. Shelf. S.* 19, 505–512. doi: 10.1016/0272-7714(84)90012-X

Ke, S., Zhang, P., Ou, S. J., Zhang, J. X., Chen, J. Y., and Zhang, J. B. (2022). Spatiotemporal nutrient patterns, composition, and implications for eutrophication mitigation in the Pearl River Estuary, China. *Estuar. Coast. Shelf. S.* 226, 107749. doi: 10.1016/j.ecss.2022.107749

Kellermeier, M., Gebauer, D., Melero-Garcia, E., Drechsler, M., Talmon, Y., Kienle, L., et al. (2012). Colloidal stabilization of calcium carbonate prenucleation clusters with silica. *Adv. Funct. Mater.* 22 (20), 4301–4311. doi: 10.1002/adfm.201200953

Kranzler, C. F., Krause, J., Brzezinski, M. A., Edwards, B. R., Biggs, W. P., Maniscalco, M., et al. (2019). Silicon limitation facilitates virus infection and mortality of marine diatoms. *Nat. Microbiol.* 4, 1790–1797. doi: 10.1038/s41564-019-0502-x

Lee, M., Park, B. S., and Baek, S. H. (2018). Tidal influences on biotic and abiotic factors in the seomjin river estuary and Gwangyang bay, Korea. *Estuar. Coasts.* 41, (4). doi: 10.1007/s12237-018-0404-9

Li, L. (2011). Effects of cage culture on nitrogen and phosphorus contents in shuidong Bay. *Merchandise Quality.* S7), 245–246. Available at: http://www.cnki.com.cn/Article/CJFDTotal-SPZN2011S7216.htm.

Li, J. C. (2021). *Influence of tidal action, typhoon and human activities on the circulation of biogenic elements in Zhanjiang Bay* (Zhanjiang: Guangdong Ocean University).

Li, B. S., Li, C. X., Jin, Y. X., Ji, P., Zhao, X. L., and He, S. (2020). Evaluation of spatial and temporal distribution of nutrient salts and eutrophication in Guanghai Bay sea. *Mar. Environ. Sci.* 39 (5), 657–663. doi: CNKI:SUN:HYHJ.0.2020-05-001

Li, J. L., Zheng, B. H., Zhang, L. S., Jin, X. W., Hu, X. P., Liu, F., et al. (2016). Eutrophication characteristics and variation analysis of major estuarine bays in China. *China Environ. Sci.* 36 (2), 506–516. doi: 10.3969/j.issn.1000-6923.2016.02.030

Lin, G. M., and Lin, X. B. (2022). Bait input altered microbial community structure and increased greenhouse gases production in coastal wetland sediment. *Water. Res.* 218 (3), 118520. doi: 10.1016/j.watres.2022.118520

Liu, Y. D. (2019). *Study on the influence of wave-generated currents on the evolution of lagoon coastal topography* (Liaoning: Dalian University of Technology).

Liu, X. F., Duan, X. Y., Tian, Y., Cao, K., Gao, F., Yin, P., et al. (2021). Nutrient changes in the water column of Sanmen Bay and its response to human activities. *Front. Mar. Geol.* 37 (5), 46–56. doi: 10.16028/j.1009-2722.2020.052

Liu, S. M., Li, R. H., Zhang., G. L., Wang., D. R., Du, Z., Herbeck, L. S., et al. (2011). The impact of anthropogenic activities on nutrient dynamics in the Tropical Wenchanghe and Wenjiaohe estuary and lagoon system in east Hainan, China. *Mar. Chem.* 125 (1-4), 49–68. doi: 10.1016/j.marchem.2011.02.003

Liu, X. H., Wang, Y. J., Shi, Y. J., Liu, D. Y., Wang, Y. X., Tian, H. L., et al. (2020). Spatial and temporal distribution of nutrients and chlorophyll-a, and their influential factors in Caofeidian coastal waters. *J. Mar. Environ. Sci.* 39, 89–98. doi: CNKI:SUN: HYHJ.0.2020-01-013

Maguire, T. J., and Fulweiler, R. W. (2017). Fate and effect of dissolved silicon within wastewater treatment effluent. *Environ. Sci. Technol.* 51 (13), 7403–7411. doi: 10.1021/acs.est.7b01276

Meirinawati, H., and Prayitno, H. B. (2021). Spatial distribution of nutrients in Maumere Bay, East Nusa Tenggara. *IOP Conf. Ser.: Earth Environ. Sci.* 890, 012006. doi: 10.1088/1755-1315/890/1/012006

Montani, S., Magni, R., and Shimamoto, M. (1998). The effect of a tidal cycle on the dynamics of nutrients in a tidal estuary in the seto inland sea, Japan. *J. Oceanogr.* 54 (1), 65–76. doi: 10.1007/BF02744382

Niu, L. X., Gelder, P.H.A.J.M., Zhang, C. K., Guan, Y. Q., and Vrijling, J. K. (2016). Physical control of phytoplankton bloom development in the coastal waters of Jiangsu (China). *Ecol. Model.* 321, 75–83. doi: 10.1016/j.ecolmodel.2015.10.008

Officer, C., and Ryther, J. (1980). The possible importance of silicon in marine eutrophication. *Mar. Ecol. Prog. Ser.* 3, 83–91. doi: 10.3354/meps003083

Pan, S. J., and Shen, Z. L. (2009). Characteristics of silicate distribution changes in the Yangtze River estuary and its adjacent waters. *Studia Marina Sinica.* 1, 10–18. doi: CNKI:SUN:HKJK.0.2009-00-005

Papush, L., Danielsson, Å., and Rahm, L. (2009). Dissolved silica budget for the Baltic Sea. *J. Sea. Res.* 62, 31–41. doi: 10.1016/j.seares.2009.03.001

Qin, Y. C., and Weng, H. X. (2006). Silicon release and its speciation distribution inthe surficial sediments of the pearl river estuary, China. *Estuar. Coast. Shelf. S.* 67 (3), 433–440. doi: 10.1016/j.ecss.2005.11.015

Qin, F. S., Yang, Z. G., Yao, S. S., and Li, S. (2014). Simulation study on the effect of comprehensive improvement project on water and sand dynamics in Shuidong Bay of Maoming City. *China Harbour Engineer.* 3, 51–56. doi: 10.7640/zggwjs201403010

Qu, F., Liu, M., Hou, L. J., Xu, S. Y., Liu, Q. M., and Ou, D. N. (2007). Changes of overlying water environmental factors and nitrogen nutrients under the influence of tidal cycle and their correlation. *Resour. Enviro. Yangtze. Basin.* 3, 345–350. doi: 10.3969/j.issn.1004-8227.2007.03.016

Qu, L. M., Yao, D., and Cong, P. F. (2006). Characteristics of nitrogen and phosphorus nutrient changes in Liaodong Bay and evaluation of potential eutrophication. *Environ. Science.* 2, 263–267. doi: 10.3321/j.issn:0250-3301.2006.02.013

Raguneau, O., Schultes, S., Bidle, K., Claquin, P., and Moriceau, B. (2006). Si and C interactions in the world ocean: Importance of ecological processes and implications for the role of diatoms in the biological pump. *Glob. Biogeochem. Cycles.* 20, (4). doi: 10.1029/2006GB002688

Redfield, A. C., Ketchum, B. H., and Richards, F. A. (1963). "The influence of organisms on the composition of seawater," in *The Sea*, vol. 2 . Ed. M. N. Hill (New York, NY, USA: John Wiley), 26–77.

Ren, M. J. (2019). Distribution characteristics of nutrient salts in the Humen River estuary of the Pearl River and their environmental impacts. *J. Water Resour. Res.* 8 (4), 371–381. doi: 10.12677/JWRR.2019.84043

Santos, I., Burnett, W. C., and Chanton, J. (2008). Nutrient biogeochemistry in a Gulf of Mexico subterranean estuary and groundwater- derived fluxes to the coastal ocean. *Limnol. Oceanogr.* 53 (2), 705–718. doi: 10.4319/lo.2008.53.2.0705

Satinder, P. S., Sunil, K. S., Ravi, B., and Vinai, K. R. (2015). Dissolved silicon and its isotopes in the water column of the Bay of Bengal: Internal cycling versus lateral transport. Geochim. Cosmochim. Acta 151, 172–191. doi: 10.1016/j.gca.2014.12.019

Shi, Z., and Huang, X. P. (2013). Structure of N, P, Si and their temporal-spatial distribution in Daya Bay, South China. Mar. Environ. Sci. 32, 916–921. doi: CNKI:SUN: HYHJ.0.2013-06-026

Shi, Y. Z., Zhang, C. X., Zhang, J. B., Chen, C. L., Zhao, L. R., and Sun, S. L. (2017). Characteristics of tidal distribution of phytoplankton and its relationship with environmental factors in the sea of Shuidong Bay. J. Ecol. 37 (18), 5981–5992. doi: 10.5846/stxb201606291286

Song, J. M. (2010). Biogeochemical Processes of Biogenic Elements in China Marginal Seas (Springer: Berlin/Heidelberg, Germany), 1–662.

Song, S. Z., Gao, L., Ge, J. Z., Guo, W. Y., and Li, D. J. (2022). Tidal effects on variations in organic and inorganic biogeochemical components in Changjiang (Yangtze River) Estuary and the adjacent East China Sea. J. Mar. Syst. 227, 103692. doi: 10.1016/j.jmarsys.2021.103692

Song, J. M., Qu, B. X., Li, X. G., Yuan, H. M., Li, N., and Duan, L. Q. (2018). Carbon sinks/sources in the Yellow and East China Seas—Air-sea interface exchange, dissolution in seawater, and burial in sediments. Sci. China Earth. 6, 1583–1593. doi: 10.1007/s11430-017-9213-6

Song, D. H., Wang, X. H., Andrew, E., and Bao, X. W. (2011). The contribution to tidal asymmetry by different combinations of tidal constituents. J. Geophys. ResOceans. 116 (C12), C12007. doi: 10.1029/2011JC007270

Su, L., Huang, Z. R., and Chen, Z. Z. (2015). Structural characteristics of phytoplankton communities in spring and autumn in Shuidong Bay. South China Fisheries Science. 11 (4), 27–33. doi: 10.3969/j.issn.2095-0780.2015.04.004

Sun, X. Y., Dong, Z. J., Zhang, W. J., Sun, X. H., Hou, C. W., Liu, Y. L., et al. (2022). Seasonal and spatial variations in nutrients under the influence of natural and anthropogenic factors in coastal waters of the northern Yellow Sea, China. Mar. Pollut. Bull. 175, 113171. doi: 10.1016/j.marpolbul.2021.113171

Sun, Y. M., and Song, J. M. (2001). Biogeochemistry of nitrogen phosphorus and silicon near the ocean sediment-seawater interface. Geol. Rev. 47, 527–534. doi: 10.16509/j.georeview.2001.05.016

Sun, P. X., Wang, B., Zhang, C. H., Wang, Z. L., and Xia, B. (2006). Relationship between nutrient distributions and eutrophication in seawater of the Laizhou Bay. J. Adv. Mar. Sci. 24, 329–335. doi: 10.3969/j.issn.1671-6647.2006.03.009

Sutton, J. N., André, L., Cardinal, D., Conley, D. J., DE, S. G. F., Dean, J., et al. (2018). A review of the stable isotope biogeochemistry of the global silicon cycle and its associated trace elements. Front. Earth Sci. 5, 112. doi: 10.3389/feart.2017.00112

Tao, W., Niu, L. X., Dong, Y. H., Fu, T., and Lou, Q. S. (2021). Nutrient pollution and its dynamic source-sink pattern in the pearl river estuary (South China). Front. Mar. Sci. 8. doi: 10.3389/fmars.2021.713907

Tréguer, P. J., and Rocha, C. L. D. L. (2013). The world ocean silica cycle. Annu. Rev. Mar. Sci. 5, 477–501. doi: 10.1146/annurev-marine-121211-172346

Turner, R. E., Rabalais, N. N., Justic, D., and Dortch, Q. (2003). Global patterns of dissolved N, P and Si in large rivers. Biogeochemistry 64, 297–317. doi: 10.1023/A:1024960007569

Uncles, R. J., and Stephens, J. A. (1996). Salt intrusion in the tweed estuary. Estuar. Coast. Shelf. S. 43, 271–293. doi: 10.1006/ecss.1996.0070

Wang, C. Y. (2019). Investigation of water quality conditions in the main bays of Zhangzhou City and evaluation of eutrophication. Fish. Res. 41 (6), 526–531. doi: 10.14012/j.cnki.fjsc.2019.06.010

Wang, Q. Q., Li, H. L., Zhang, Y., Wang, X. J., Xiao, K., Zhang, X. L., et al. (2020). Submarine groundwater discharge and its implication for nutrient budgets in the western Bohai Bay, China. J. Environ. Radioactiv. 212, 106132. doi: 10.1016/j.jenvrad.2019.106132

Wang, F., Lu, Z., Wang, Y., Yan, R., and Chen, N. (2023). Porewater exchange drives the dissolved silicate export across the wetland-estuarine continuum. Front. Mar. Sci. 10, 812. doi: 10.3389/fmars.2023.1206776

Wu, B., and Liu, S. M. (2020). Dissolution kinetics of biogenic silica and the recalculated silicon balance of the East China Sea. Sci. Total. Environ. 743, 140552. doi: 10.1016/j.scitotenv.2020.140552

Wu, H., Zhu, J. R., Shen, J., and Wang, H. (2011). Tidal modulation on the changjiang river plume in summer. J. Geophys. Res-Oceans. 116 (8), C08017. doi: 10.1029/2011JC007209

Xie, L. P., Pu, X. M., Sun, X., and Wang, B. D. (2013). Analysis on the temporal and spatial distribution of nutrients and the influence factors in Rongcheng Bay. Mar. Sci. Bull. 32, 19–27. doi: CNKI:SUN:HUTB.0.2013-01-005

Yang, B., Gao, X., Zhao, J., Lu, Y., and Gao, T. (2020). Biogeochemistry of dissolved inorganic nutrients in an oligotrophic coastal mariculture region of the Northern Shandong Peninsula, North Yellow Sea. Mar. Pollut. Bull. 150, 110693. doi: 10.1016/j.marpolbul.2019.110693

Yang, L. Z., Liu, H. K., Ren, J., and Yu, F. H. (2011). Preliminary study on twoway jet system in the near-shore waters of Shuidong bay. Acta Scientiarum. Naturalium. Universitatis. Sunyatseni. 50 (2), 116–119. doi: CNKI:SUN:ZSDZ.0.2011-02-025

Yin, K. D., and Harrison, P. (2000). Influences of flood and ebb tides on nutrient fluxes and chlorophyll on an intertidal flat. Mar. Ecol. Prog. Ser. 196 (3), 75–85. doi: 10.3354/meps196075

You, L. P., Zhao, Y. Y., Sun, S., Su, B., Ma, Y. Q., Wang, L. M., et al. (2021). Nutrient salt structure and limiting characteristics of Laizhou Bay in spring and summer 2018. Prog. Fish. Sci. 42 (6), 15–24. doi: 10.19663/j.issn2095-9869.20200715001

Yu, J. T., and Chen, Z. S. (2010). Analysis of power depositional environment in Shuidong Bay, western Guangdong, China. Mar. Geological Dynamics. 26 (5), 34–38. doi: 10.16028/j.1009-2722.2010.05.001

Yuan, H., Song, J., Xing, J., Li, X., Li, N., Duan, L., et al. (2018). Spatial and seasonal variations, partitioning and fluxes of dissolved and particulate nutrients in Jiaozhou Bay. Cont. Shelf. Res. 171, 140–149. doi: 10.1016/j.csr.2018.11.004

Zang, J. Y., Wang, H., Liu, J., Yu, Z. G., Wu, N., and Ran, X. B. (2020). Advances in the study of biogenic silicon composition and impact on silicon cycle. Adv. Mar. Sci. 1, 11–20. doi: CNKI:SUN:HBHH.0.2020-01-002

Zhang, X. S. (2015). Numerical analysis of flushing and siltation evolution in a narrow and semi-enclosed Silty bay (Zhanjiang: Ocean University of China).

Zhang, P., Chen, Y., Peng, C. H., Dai, P. D., Lai, J. Y., Zhao, L. R., et al. (2020a). Spatiotemporal variation, composition of DIN and its contribution to eutrophication in coastal waters adjacent to Hainan Island, China. Reg. Stud. Mar. Sci. 37, 101332. doi: 10.1016/j.rsma.2020.101332

Zhang, P., Dai, P. D., Zhang, J. B., Li, J. X., Zhao, H., and Song, Z. G. (2021). Spatiotemporal variation, speciation, and transport flux of TDP in Leizhou Peninsula coastal waters, South China Sea. Mar. pollut. Bull. 167, 112284. doi: 10.1016/j.marpolbul.2021.112284

Zhang, P., Luo, W. S., Fu, M. J., Zhang, J. B., Cheng, M. Y., and Xie, J. L. (2022). Effects of tidal variations on total nitrogen concentration, speciation, and exchange flux in the Shuidong Bay coastal water, South China Sea. Front. Mar. Sci. 9. doi: 10.3389/fmars.2022.961560

Zhang, H. B., Pei, S. F., Zhu, Y. X., Wang, L. S., Shi, X. Y., Ye, S. Y., et al. (2018). Structural characteristics of nutrient salts in Bohai Bay in early summer and analysis of their limitation status. China. J. Environ. Sci. 38 (9), 3524–3530. doi: CNKI:SUN: ZGHJ.0.2018-09-045

Zhang, L., Ren, G. Y., Baoleerqimuge,, Xu, B., and Yu, J. J. (2017a). Climatology and change of the South China Sea surface temperature based on satellite observations. Climate Change Res. 13 (3), 189–197. doi: 10.12006/j.issn.1673-1719.2016.200

Zhang, P., Ruan, H. M., Dai, P. D., Zhao, L. R., and Zhang, J. B. (2020b). Spatiotemporal river flux and composition of nutrients affecting adjacent coastal water quality in Hainan Island, China. J. Hydrol 591, 125293. doi: 10.1016/j.jhydrol.2020.125293

Zhang, P., Su, Y., Liang, S. K., Li, K. Q., Li, Y. B., and Wang, X. L. (2017b). Assessment of long-term water quality variation afffected by high-intensity land-based inputs and land reclamation in Jiaozhou Bay, China. Ecol. Indic. 75, 210–219. doi: 10.1016/j.ecolind.2016.12.035

Zhang, P., Wei, L. R., Lai, J. Y., Dai, P. D., Chen, Y., and Zhang, J. B. (2019). Concentration, composition and fluxes of land based nitrogen and phosphorus source pollutants input into Zhanjiang Bay in Summer. J. Guangdong Ocean Univ. 39, 46–55. doi: 10.3969/j.issn.1673-9159.2019.04.000

Zhang, P., Xu, J. L., Zhang, J. B., Li, J. X., Zhang, Y. C., Li, Y., et al. (2020c). Spatiotemporal dissolved silicate variation, sources, and behavior in the eutrophic Zhanjiang bay, China. Water 12, 3586–3586. doi: 10.3390/w12123586

Zhao, Y. F., Zhao, Z. X., and Sun, X. X. (2020). Data set of nutrient structure and phytoplankton growth limiting factors in Jiaozhou Bay waters from 1997-2010. China Scientific Data (Chinese and English online version). 5 (1), 31–40. doi: 10.11922/csdata.2019.0056.zh

Zhou, M. (2021). Study on the spatial and temporal distribution of chlorophyll a and nutrient salts and potential eutrophication in Zhanjiang Bay sea surface in autumn 2017-2020 (Zhanjiang: Guangdong Ocean University).

Zhou, M., and Zhao, H. (2021). Characteristics of spatial and temporal distribution of chlorophyll a concentration in Zhanjiang Bay in autumn and its correlation with environmental factors. J. Guangdong Ocean University. 41 (6), 25–35. doi: 10.3969/j.issn.1673-9159.2021.06.004

Zhu, H. G. (2017). Advances in the biogeochemistry of silica in estuarine coastal zones. Jiangsu Water Resour. 10, 32–36. doi: 10.16310/j.cnki.jssl.2017.10.008